

Simulation of Auxin Accumulation and Transport in a Plant Root

Introduction: Plant roots have an outstanding ability to grow in the direction of gravity [1,2](Fig.1). Bending of the root tip in the preferred direction is achieved by asymmetric cell growth on the opposite sides of the root, dictated by asymmetrical distribution of the **hormone auxin**(IAA), which inhibits cell elongation (Fig.2). Mechanism of inhibition is not known and its experimental studies involve external auxin application and evaluation of root growth rate [3]. We simulate dynamics of auxin uptake from the media to deduce contribution of auxin transport to the timing of growth inhibition response.

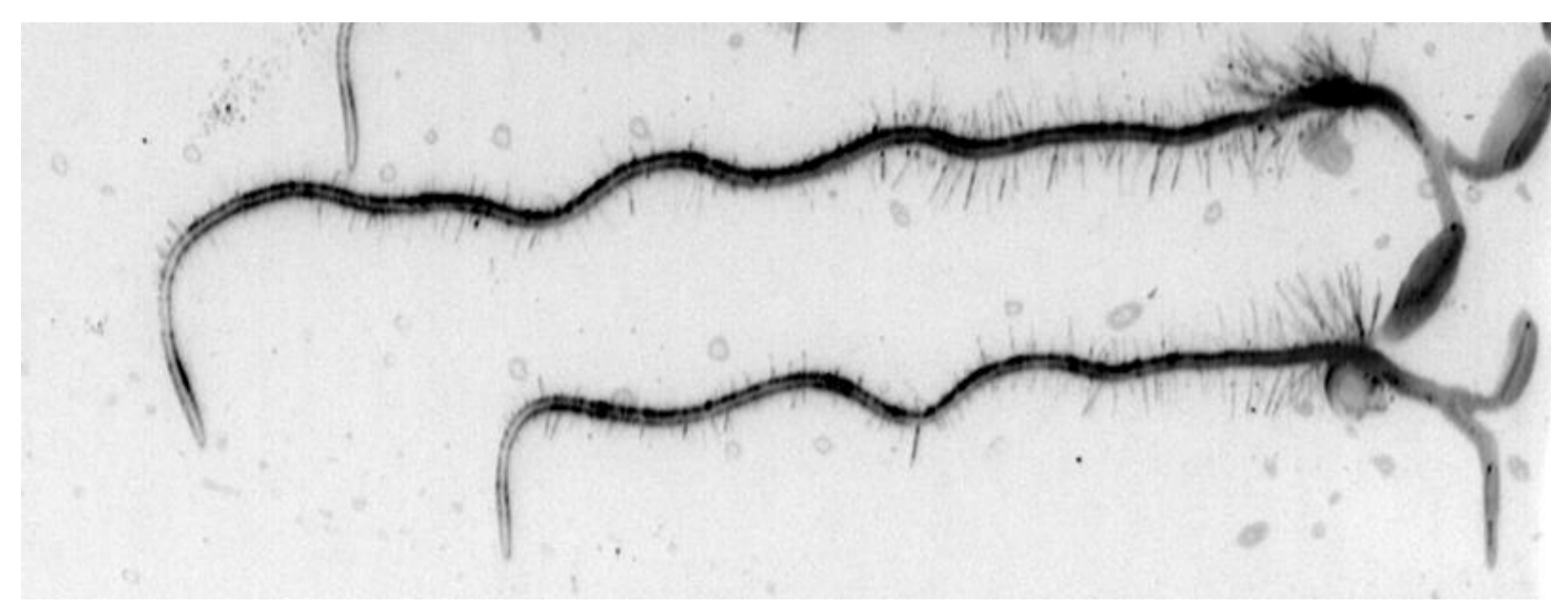


Figure 1. Gravitropism: growing tip of the plant root bends down after it is placed horizontally because →

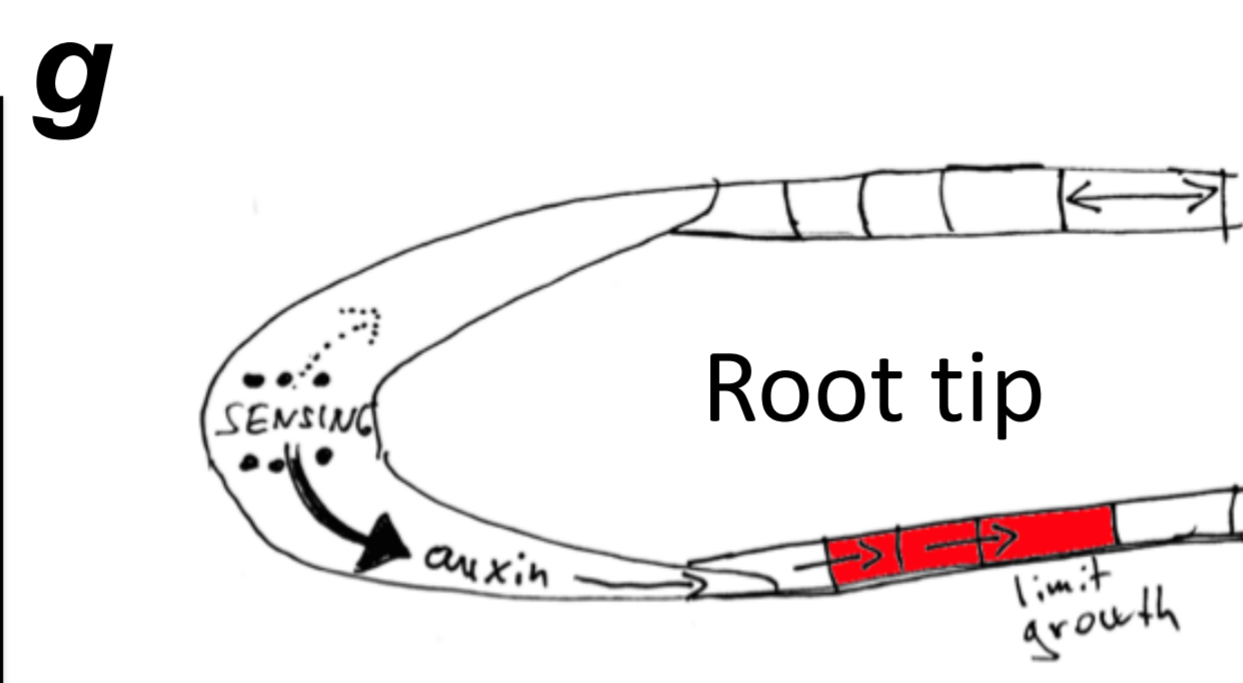


Figure 2. Auxin accumulates on the lower side of the root and stops cell growth

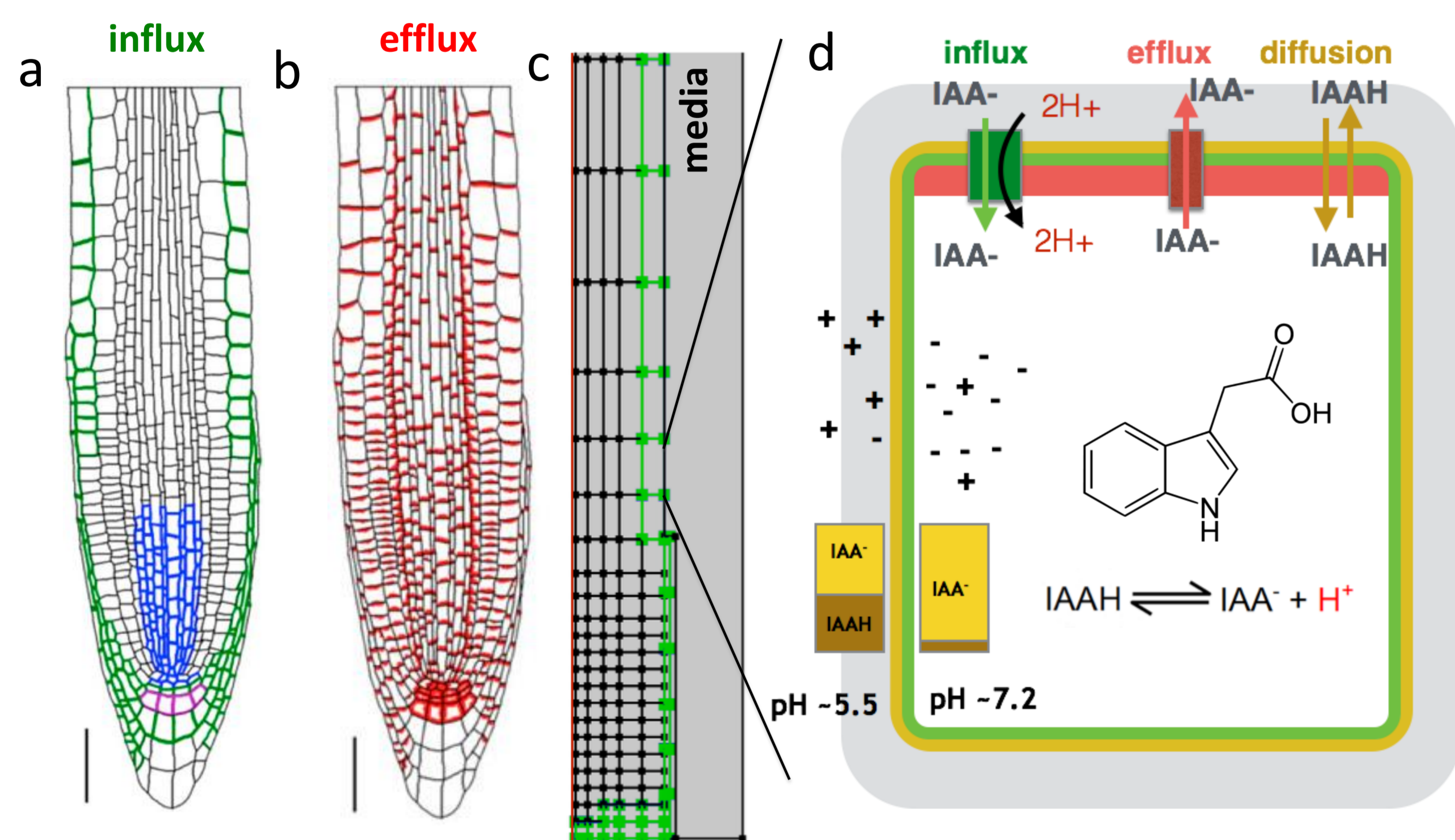


Figure 3. Localization of (a) influx transporters (**AUX1 & LAX**) and (b) polarized efflux transporters (**PINs**) (from ref.[2]). (c) Model geometry with influx carriers in green. (d) Scheme of IAA fluxes in a cell: anion form IAA^- is taken inside by influx carriers against membrane potential and outside by efflux carriers; protonated form $IAAH$ transports by diffusion. Fluxes depend on pH difference across the membrane as well as on the membrane potential.

Methods: Geometry of our 2D-axisymmetrical finite-element model of the *Arabidopsis* root apex comprises of individual cells, separated by a thin layer of extracellular space. Auxin concentration ($IAA(x,t)$) is determined by mass conservation law, comprising 1) **diffusion** of IAA inside the cell/wall compartments and 2) **fluxes** across the membranes (=molecules passed through membrane per unit time per unit area), which are determined by **diffusion**, **influx** and **efflux** transporters (with permeabilities P_{diff} , P_{inf} , P_{eff} defined on membranes with respect to transporters localization)[2] (Fig.3). Flux $J_{wall \rightarrow cell} = J_{diff} + J_{influx} + J_{efflux}$

$$J_{diff} = P_{diff}(\alpha_1[IAA_{wall}] - \beta_1[IAA_{cell}])$$

$$J_{influx} = P_{inf}(\alpha_2[IAA_{wall}] - \beta_2[IAA_{cell}]) \quad \alpha_i, \beta_i = F(pH, V_{mem})$$

$$J_{efflux} = P_{eff}(\alpha_3[IAA_{wall}] - \beta_3[IAA_{cell}])$$

Outer domain simulates media. Transport equations are solved using the Chemical Reaction Engineering Module in COMSOL Multiphysics® to compute intracellular auxin concentration (IAA_{cell}) in space and time depending on auxin concentration in media ($IAA_{external}$).

Results: Auxin accumulation shows highest concentration in the outer layer (epidermis) and an ascendant gradient along the root (Fig.4) because auxin is pumped up by efflux carriers, that are localized solely on the upper membrane, whereas influx carriers are distributed evenly on the membrane (Fig.3ab).

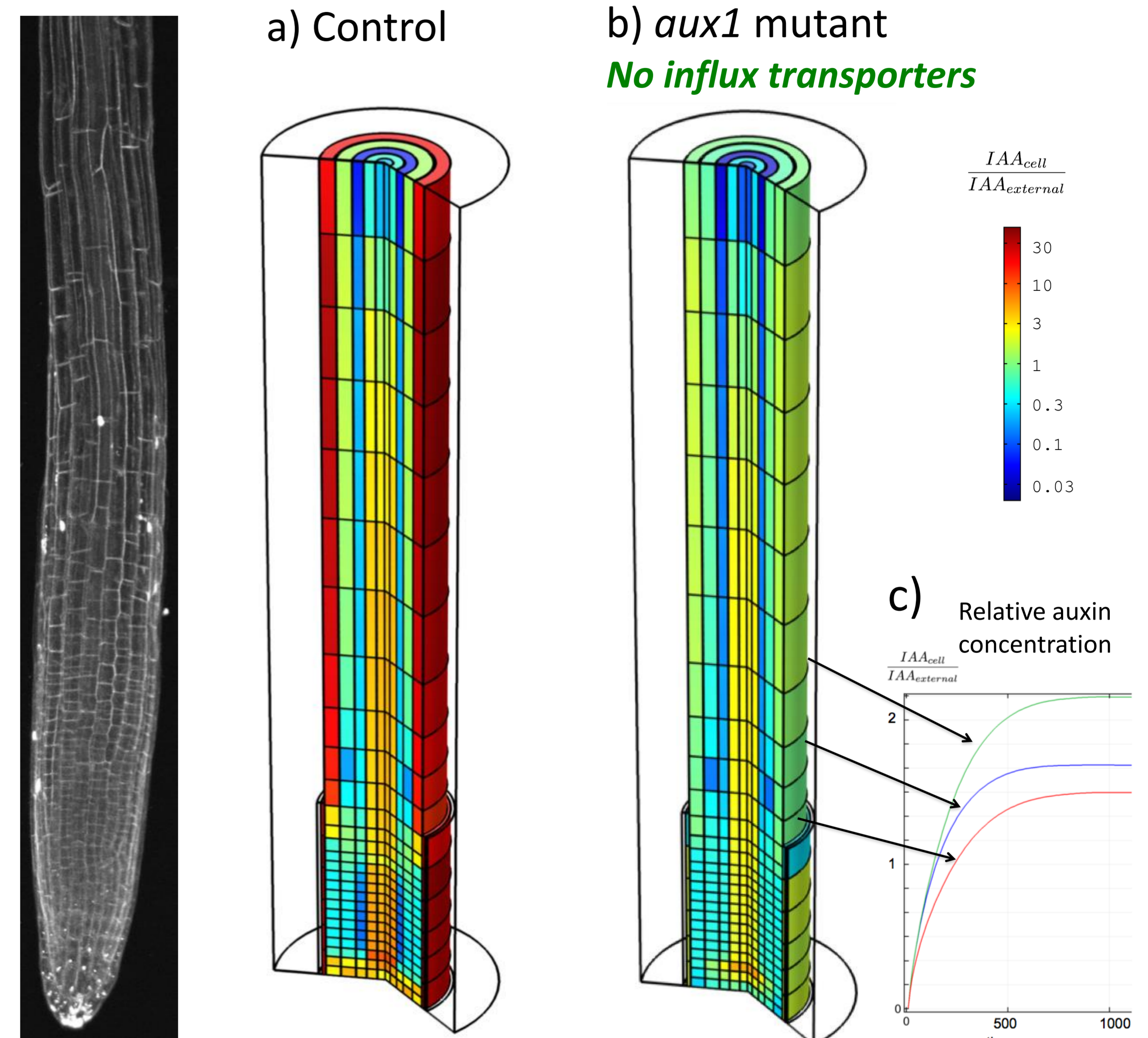


Figure 4. Steady state IAA concentration ($IAA_{cell}/IAA_{external}$) in (a) control root, (b) *aux1* mutant lacking **AUX1** transporters. (c) $IAA(t)$ dynamics for 3 individual epidermal cells.

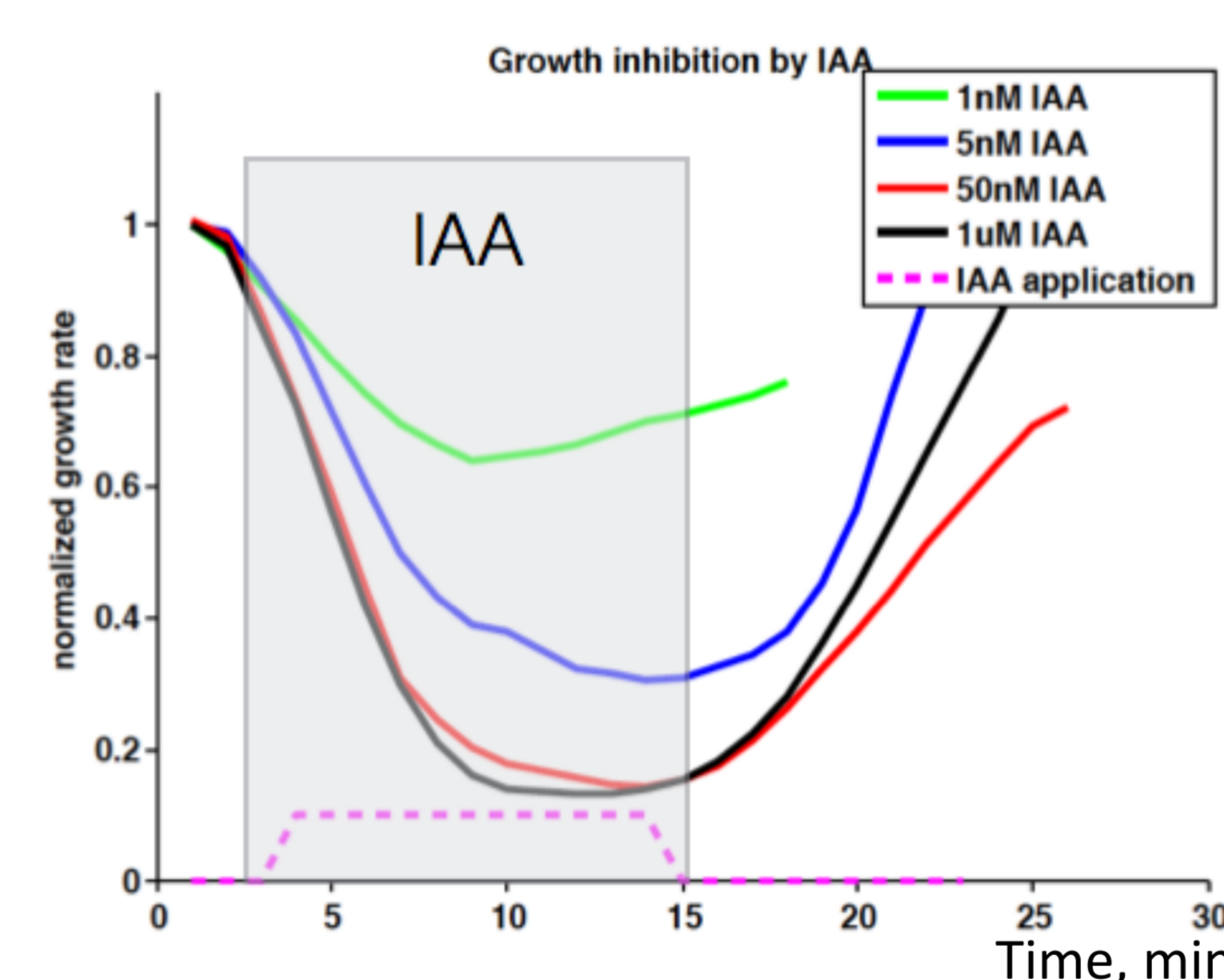


Figure 5. Experimental growth rate response is concentration-dependent with saturation for >50nM IAA

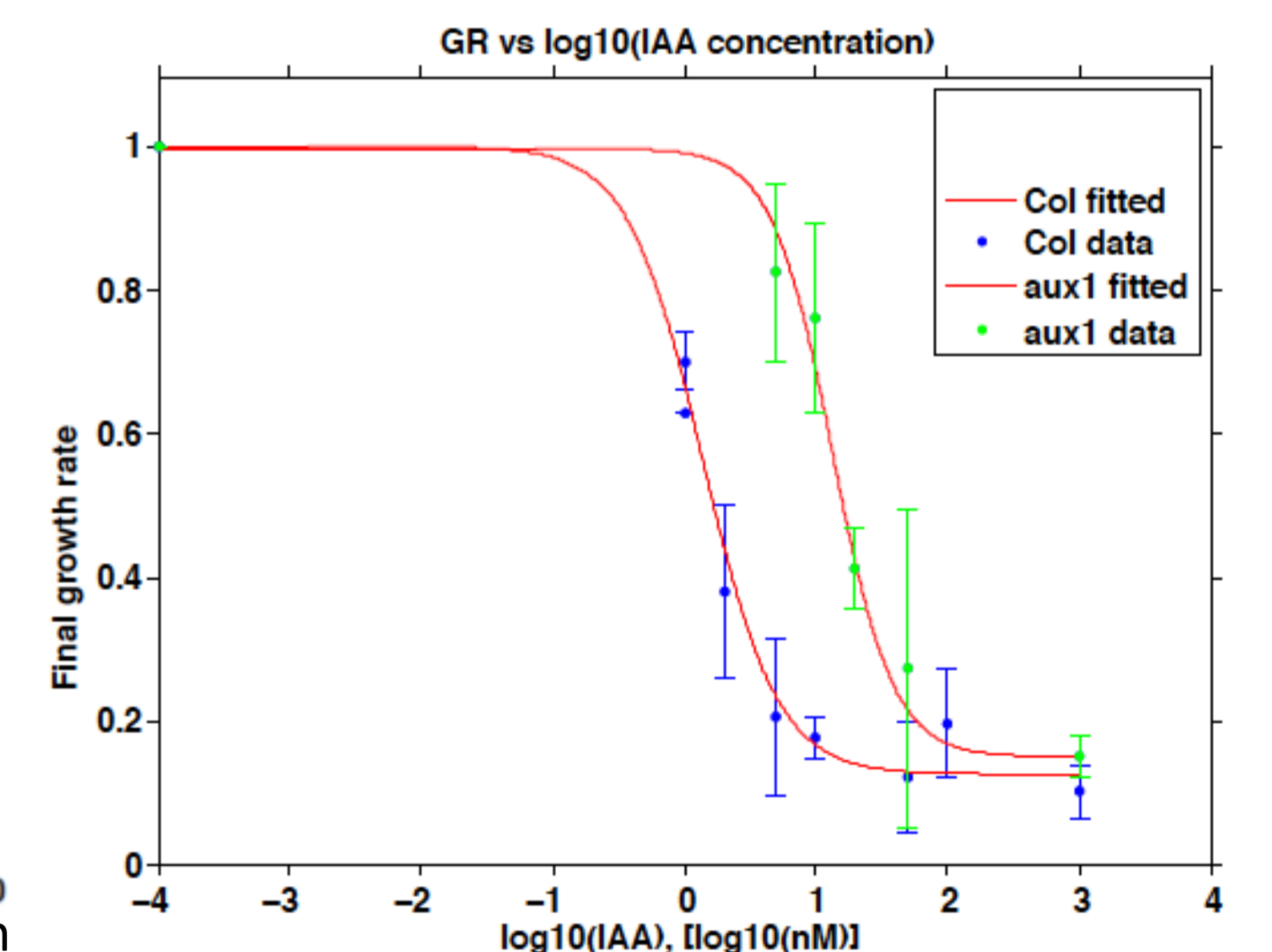


Figure 6. In *aux1* mutant dose response is shifted to ~10 times higher concentrations of IAA

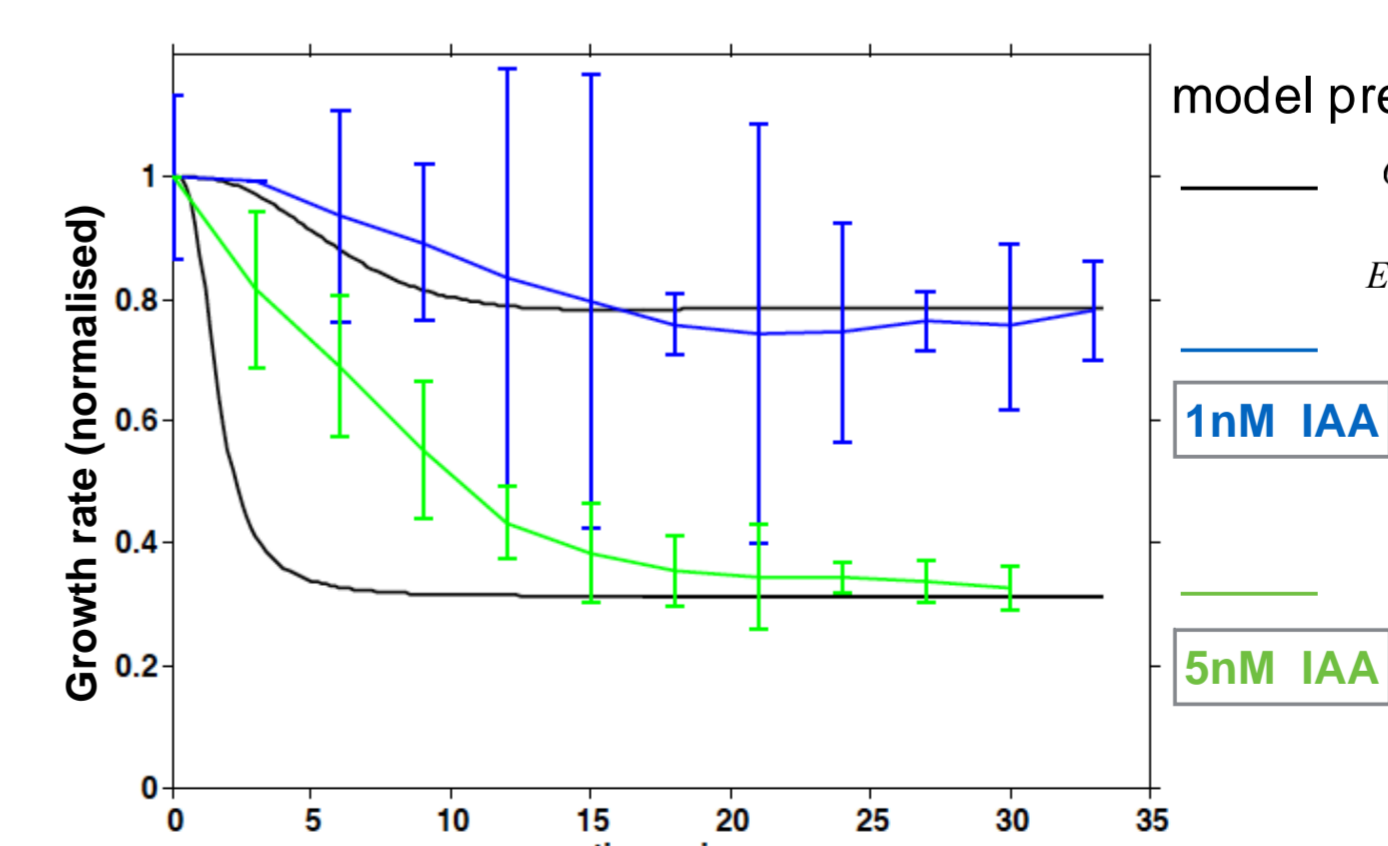


Figure 7. Auxin growth response kinetics: experimental growth rate ($GR(t)$) and prediction from model derived $IAA(t)$ in case if growth response would be auxin-transport-limited.

Conclusions: Intracellular steady state IAA concentration is proportional to IAA in the media for $[IAA_{external}] > 5nM$. Growth inhibition is limited by signaling pathway reactions rate, not by auxin transport. Our model is used to compare growth inhibition response to IAA in mutants to dissect contribution of IAA transport.

References:

1. R. Swarup *et al.*, *Nat. Cell Biol.*, 7, (11), pp. 1057–1065, 2005.
2. L. R. Band *et al.*, *Plant Cell*, 26, no. 3, pp. 862–875, 2014.
3. von Wangenheim D, Hauschild R, Fendrych M, Barone V, Friml J (2017) *eLife* 6: e26792
4. Fendrych M, Leung J & Friml J (2016) *eLife* 5:e19048